DOI: 10.12923/cipms-2026-0022 Curr. Issues Pharm. Med. Sci., Vol. 39, No. 3, Pages 141-149

Current Issues in Pharmacy and Medical Sciences
Formerly ANNALES UNIVERSITATIS MARIAE CURIE-SKLODOWSKA, SECTIO DDD, PHARMACIA

journal homepage: https://czasopisma.umlub.pl/curipms



Formulation and evaluation of fexofenadine hydrochloride-loaded niosomes for topical delivery

H.S. Lavanya[1,2], H.N. Shivakumar[1,2*], Bindu Banakar[1,2], Rushikesh Shinde[1,2]

[1] Centre of Innovative Science and Engineering Education, Department of Pharmaceutics, KLE College of Pharmacy, Rajajinagar, Bengaluru 560010, India
[2] KLE Academy of Higher Education and Research (Deemed-to-be-University), Belagavi 590010, India

ARTICLE INFO

Received 20 February 2026
Accepted 09 June 2026

Keywords:
fexofenadine hydrochloride;
chronic idiopathic urticaria;
niosomes;
ex vivo permeation;
ultra-deformable.

ABSTRACT

Fexofenadine hydrochloride (FEX HCl), a second-generation antihistamine, is widely used in the treatment of chronic idiopathic urticaria (CIU). The present study aimed to develop and optimize FEX-loaded niosomes to enhance topical drug delivery for the management of CIU. Eight batches of niosomes were prepared using a 2^3 full factorial design by the ethanol evaporation method. The percentage entrapment efficiency (%EE) and percentage *in vitro* drug release at 8 h (%DR) of the model niosomal formulations ranged from 53.67 ± 0.16% to 77.32 ± 0.20% and from 42.80 ± 0.25% to 64.32 ± 0.24%, respectively. The optimized niosomal batch exhibited a reduced particle size of 160 ± 7.3 nm, good colloidal stability, with a zeta potential of −28.9 ± 5.5 mV, and high entrapment efficiency of 77.32 ± 0.20%. Scanning electron microscopy indicated the spherical morphology and nanoscale size of the niosomes, whereas differential scanning calorimetry and X-ray diffractometry confirmed the presence of the drug in a molecular state within the niosomal bilayer. The optimized formulation was incorporated into a Carbopol-based gel and evaluated for physical properties, *in vitro* drug release, and *ex vivo* skin permeation. The niosomal gel showed prolonged drug release, with 63.57 ± 2.21% released within 8 h, compared with the drug solution. *Ex vivo* studies demonstrated significantly enhanced ($p < 0.0001$) skin permeation, with 51.97 ± 0.28 μg/cm³ drug permeated from the niosomal gel compared with 30.00 ± 0.28 μg/cm³ from the FEX gel. These results indicate that niosomes may be promising carriers for the topical delivery of FEX in the treatment of CIU.

INTRODUCTION

Urticaria is characterized by the sudden onset of itchy wheals, which may occur either alone or in association with angioedema [1]. Angioedema is characterized by deeper dermal and subcutaneous swelling, usually lasts longer than wheals, and may also occur alone or in association with urticaria [2]. Urticaria results from plasma leakage from superficial blood vessels and manifests as intensely itchy wheals that usually resolve without scarring [3]. Second-generation antihistamines are the first-line treatment for chronic spontaneous urticaria because of their favorable safety profile [1].

Fexofenadine hydrochloride (FEX HCl) is a non-sedating, peripherally selective H1-antihistamine that can be administered once or twice daily for long-term treatment because of its prolonged half-life [4]. However, despite its therapeutic benefits, FEX HCl has low oral bioavailability, approximately 33%, due to poor intestinal permeability and P-glycoprotein-mediated efflux [5]. Moreover, FEX HCl is relatively hydrophilic (log P: 0.49), as it is primarily zwitterionic at physiological pH, which may contribute to poor oral absorption [6].

In this regard, topical delivery of FEX HCl may be advantageous because it can bypass gastrointestinal barriers, including pH changes, enzymatic degradation, and first-pass metabolism. In addition, topical products can be applied over a large surface area and may provide direct access to the target site [7]. Among topical formulations, gels are preferred because of their non-greasy texture and improved patient compliance and acceptability [8].

* **Corresponding author**
e-mail: shivakumarhn@klepharmblr.org,
shivakumarhn@gmail.com

© 2026 Author(s). This is an open access article distributed under the Creative Commons Attribution-NonComercial-No Derivs licence (http://creativecommons.org/licenses/by-nc-nd/4.0/)

Niosomes are innovative vesicular systems based on non-ionic surfactants that have attracted considerable attention among nanocarriers because of their favorable biocompatibility, high stability, and ability to encapsulate both lipophilic and hydrophilic drugs [9]. Niosomes are known to enhance the absorption of hydrophilic drugs following topical application [10]. Designing niosomes at the nanoscale is known to improve the efficacy of topical therapy [11].

The current study primarily aimed to evaluate the effects of formulation and processing parameters, including cholesterol level, Span 60 level, and sonication time, on critical quality attributes such as percentage entrapment efficiency and percentage drug release using a 2^3 factorial design. The second aim was to optimize these parameters to obtain a niosomal formulation with the most desirable quality attributes. Third, the optimized FEX HCl-loaded niosomal batch was characterized for particle size, polydispersity index, and zeta potential. In addition, the optimized batch was evaluated for surface topography and the solid-state characteristics of the drug. The niosomes were then incorporated into a Carbopol-based gel and subjected to ex vivo permeation studies. To the best of our knowledge, the present investigation represents a novel approach to the development of a niosomal gel for the topical delivery of FEX HCl, as no such study has previously been reported for this drug.

MATERIALS AND METHODS

Materials

FEX HCl was procured from Dham Tech Pharma, India. Cholesterol, Span 60, and triethanolamine were procured from Simson Pharma Limited, Maharashtra, India. Ethanol was procured from Yarrow Chemicals, Mumbai, India. Potassium dihydrogen orthophosphate and sodium hydroxide were procured from Hi-Media Laboratories, India, and SD Fine-Chem Limited, India, respectively. Carbopol 940 was procured from SD Fine-Chem Limited, India.

Methodology

1. Calibration curve of fexofenadine hydrochloride

A primary stock solution was prepared by dissolving 10 mg of FEX HCl in 10 mL of ethanol, resulting in a concentration of 1000 µg/mL. This solution was subsequently diluted to obtain a secondary stock solution of 100 µg/mL. Standard concentrations of 2, 4, 6, 8, and 10 µg/mL were prepared from the secondary stock solution by diluting aliquots of 0.2, 0.4, 0.6, 0.8, and 1.0 mL to 10 mL with phosphate buffer (pH 7.4).

A UV spectrophotometer was used to scan the primary stock solution over the wavelength range of 200-800 nm, using phosphate buffer (pH 7.4) as the reference blank. The selected wavelength was then used to measure the absorbance of the prepared standard solutions. Absorbance was plotted against concentration to construct the calibration curve [12].

2. Preparation of Niosomes

FEX HCl-loaded niosomes were prepared using the ethanol injection method. To prepare the organic phase, accurately weighed amounts of FEX HCl, cholesterol, and Span 60 were dissolved in ethanol and heated to 60°C. For the aqueous phase, PBS (pH 7.4) was gradually heated to 60°C. Under magnetic stirring at 400 rpm and controlled temperature conditions, 3 mL of the organic phase was gradually added to 25 mL of the aqueous phase. After ethanol evaporation using a rotary vacuum evaporator set at 50°C, the resulting dispersion was bath-sonicated for 20 min at 65% amplitude [13]. The various steps involved in the preparation of FEX HCl-loaded niosomes are shown in Figure 1. Preliminary investigations indicated that three variables, namely the amount of cholesterol (X1), the amount of Span 60 (X2), and sonication time (X3), were varied at two levels, as shown in Table 1. The batches prepared using a 2^3 full factorial design are presented in Table 2.

Table 1. Levels of variables in the 2^3 full factorial design

Independent variables	Low (-1)	High (+1)
X1: Cholesterol (%w/v)	25 mg	75 mg
X2: Span 60 (%w/v)	25 mg	75 mg
X3: Sonication time	3 min	5 min
Dependent variables	**Desire Response**	
Y1: Entrapment efficiency (%)	Maximum	
Y2: *In vitro* drug release at 8 h (%)	Maximum	

Table 2. Fexofenadine-loaded niosomal batches prepared using the 2^3 full factorial design

Runs	Independent variable		
	X1 (%w/v)	X2 (%w/v)	X3 (min)
1	75	25	5
2	25	25	3
3	75	75	5
4	25	75	3
5	25	75	5
6	75	25	3
7	75	75	3
8	25	25	5

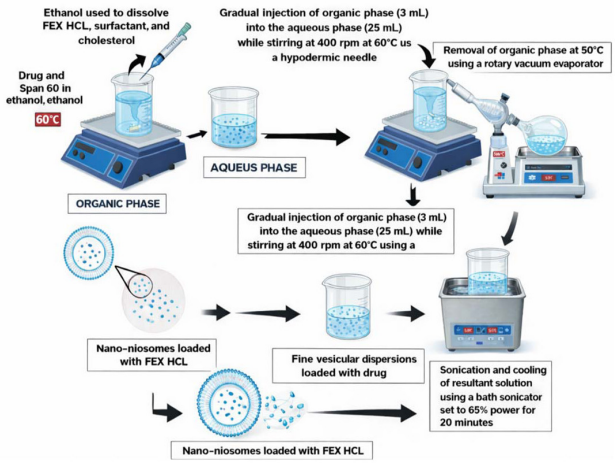


Figure 1. Schematic representation of the formulation process for fexofenadine hydrochloride-loaded niosomes using the ethanol injection method

Regression analysis

The optimal formulation was identified using Design-Expert software, version 13, based on the desirability function. Optimization was performed to select the formulation with the highest percentage entrapment efficiency (%EE; Y1) and the highest *in vitro* drug release value (Y2). The solution with a desirability value close to 1 was selected. The selected formulation was prepared, characterized, and compared with the predicted results to verify the effectiveness of the model.

The data were statistically evaluated using factorial analysis of variance (ANOVA) in Design-Expert software, version 13. The resulting polynomial equation for the factorial design is shown in Equation 1:

$$Y = ß_0 + ß_1X_1 + ß_2X_2 + ß_3X_3 + \beta_{12}X_1X_2 + \beta_{13}X_1X_3 + \beta_{23}X_2X_3 \quad (1)$$

The equation generated after statistical analysis demonstrated the quantitative effects of the independent variables (X1, X2, and X3) on the response variable (Y). The regression coefficients β_i (i = 1, 2, 3) indicate the relative significance of each independent variable in the equation, whereas β_{ij} (i = 1, 2, 3; j = 1, 2, 3) represents the interaction between factors. The sign and magnitude of each coefficient indicate whether the factor has a negative or positive effect on the response Y.

The best-fitting model was selected based on several criteria, including standard deviation, correlation coefficient, predicted residual sum of squares, and 3D response surface plots generated using Design-Expert software [14,15].

Optimization of the dependent variables

1. Entrapment efficiency

To evaluate the entrapment efficiency of FEX HCl in the niosomal dispersion, the liquid supernatant was separated from the sediment after ultracentrifugation (Eltek Instruments, India) at 15,000 rpm and 4°C for 30 min. The absorbance of the sediment and supernatant was measured at 220 nm for FEX HCl using UV spectroscopy (Shimadzu 1900i, Japan). The formula used to calculate entrapment efficiency (EE) is shown in Equation 2 [16]:

$$\%EE = \frac{\text{Amount of drug in the sediment}}{\text{Amount in supernatant} + \text{Amount in sediment}} \times 100 \quad (2)$$

2. *In vitro* drug release studies

The *in vitro* drug release of the FEX niosomal formulation was determined using the dialysis method. The colloidal dispersion of FEX HCl was placed in dialysis tubing and suspended with clamps in 100 mL of PBS (pH 7.4). Samples of approximately 1 mL were withdrawn for analysis at 1, 2, 3, 4, 5, 6, 7, and 8 h. The volume of the drug release medium was maintained at 100 mL by replacing each withdrawn sample with an equal volume of fresh medium while stirring with a magnetic stirrer at 200 rpm. The withdrawn samples were analyzed using a UV-visible spectrophotometer at 220 nm, and the percentage of drug released from the niosomal formulation was determined using the membrane diffusion method [17].

The *in vitro* dissolution data of the eight formulations were analyzed using various kinetic models, including zero-order, first-order, Higuchi, and Korsmeyer-Peppas models, to characterize the drug release mechanism. The release model with the highest correlation coefficient (R^2) was considered to best describe the predominant drug release behavior of the formulation [18].

Characterization of optimized niosomes

1. Particle size, polydispersity index, and zeta potential

The particle size of the optimized niosomal formulation was determined by dynamic light scattering using a Zetasizer (Horiba SZ-100, Japan). Before measurement, the dispersion was diluted tenfold with phosphate-buffered saline (PBS, pH 7.4). A diluted sample (1 mL) was placed in a polystyrene cuvette to determine particle size and the polydispersity index (PDI). Particle size was expressed as the volume-equivalent spherical diameter.

The zeta potential of FEX-loaded niosomes was measured using a Zetasizer (Horiba SZ-100, Japan). The samples were diluted with distilled water at a 1:1 ratio. To assess zeta potential, the samples were transferred to cuvettes and analysed using the differential laser scattering technique [19].

2. Fourier transform infrared spectroscopy

Drug-excipient compatibility was evaluated using a Fourier transform infrared (FT-IR) spectrophotometer (Jasco FT/IR-460 Plus spectrometer, Tokyo, Japan). FT-IR spectra of FEX HCl, the physical mixture, and the formulations were obtained after uniform blending of the samples with KBr using a glass mortar. The prepared mixtures were placed in a diffuse reflectance sample holder and exposed to infrared radiation. Spectra were recorded over the range of 500-4000 cm^{-1} [20].

3. Differential Scanning Calorimetry

Differential Scanning Calorimetry (DSC) was performed using a differential scanning calorimeter (Mettler Toledo, Germany). The samples were placed in aluminum pans and heated under a nitrogen atmosphere at a flow rate of 100 mL/min and a heating rate of 10°C/min. Data were acquired over a temperature range of 30-300°C, based on the melting point of FEX HCl [21].

4. X-ray diffraction

Powder X-ray diffraction (PXRD) analysis was performed using an X-ray diffractometer (Bruker D8 Advance, Germany) to examine the crystalline characteristics of FEX HCl, excipients, and the niosomal formulation. XRD data were collected using Cu Kα radiation at an operating voltage of 40 kV, a current of 40 mA, and a scanning speed of 0.5 s per step.

Diffractograms of the physical mixture, cholesterol, Span 60, FEX HCl, and the freeze-dried niosomal formulation were recorded. Powdered samples were placed in the sample holder, and diffraction patterns were obtained under the selected scanning conditions. Characteristic diffraction peaks were used to identify the phases and degree of crystallinity of the excipients and to evaluate the

crystalline state of FEX HCl within the niosomal system [22].

5. Morphology of niosomes

The surface morphology of the optimized FEX-loaded niosomal formulation was evaluated using scanning electron microscopy (SEM). Dried niosomes were mounted on aluminum sample stubs using double-sided adhesive tape and vacuum-coated with gold to make the samples electrically conductive. The samples were then examined using a scanning electron microscope (Carl Zeiss Supra 55) [23].

Energy-dispersive X-ray spectroscopy (EDX) analysis was performed at an accelerating voltage of 15 kV and a current of 12 mA to investigate the presence and distribution of carbon, oxygen, sodium, phosphorus, sulfur, and potassium atoms in the formulation [24].

Preparation of niosomal gel

The gel base, composed of Carbopol 940, triethanolamine, and distilled water q.s. to 50 mL, was mixed with the optimized batch of niosomal dispersion prepared using the optimal surfactant ratio, as shown in Table 3 [25].

Table 3. Composition of fexofenadine hydrochloride niosomal gel

Sr. no.	Ingredient	Quantity
1	Carbopol 940	1% w/v
2	Niosomal dispersion	10% v/v
3	Triethanolamine	0.4% v/v
4	Purified water	q.s. to 50 mL

Characterization of niosomal gel

1. pH

The pH of the FEX HCl gel formulation was measured using a digital pH meter. Before analysis, the gel was diluted with distilled water. The instrument was calibrated prior to measurement. Measurements were performed in triplicate to obtain the mean pH value and ensure consistency. The electrode was rinsed thoroughly between readings to avoid contamination [26].

2. Spreadability test

The spreadability of the niosomal gel was assessed 24 h after preparation at 37 ± 1°C to simulate physiological conditions. Briefly, 1 g of the formulation was placed on a glass plate and covered with another glass plate to apply pressure. The time required for the gel to spread uniformly and cover the entire surface of the plate was recorded. The experiment was performed in triplicate [27].

3. *Ex vivo* permeation studies

Franz diffusion cells were used for the *ex vivo* skin permeation study of the FEX HCl-loaded niosomal gel formulation and the control gel (FEX gel) at the same concentration (0.2% w/v). Phosphate buffer (pH 7.4) was added to the receptor compartment and continuously stirred at 100 rpm, while the system temperature was maintained at 37 ± 2°C throughout the experiment.

Abdominal skin excised from male rats was used for the study. The skin was mounted between the donor and receptor compartments, with the stratum corneum facing the donor chamber and the dermal side in contact with the receptor medium. The niosomal gel formulation was applied to the donor compartment. At predetermined time intervals (1, 2, 3, 4, 5, 6, 7, and 8 h), aliquots were withdrawn from the receptor compartment and analyzed using a UV-visible spectrophotometer (Shimadzu 1900i, Japan) at 220 nm [28].

RESULTS AND DISCUSSION

Fexofenadine hydrochloride (FEX HCl) (Figure 2) is a selective histamine H1-receptor antagonist and an active metabolite of terfenadine. Its chemical name is (RS)-2-[4-[1-hydroxy-4-[4-(hydroxydiphenylmethyl)piperidyl]butyl] phenyl]-2-methylpropanoic acid. FEX is classified as a second-generation antihistamine. On February 25, 2000, the FDA approved the use of fexofenadine for the management of seasonal allergic rhinitis and chronic urticaria.

FEX HCl exhibits poor permeability due to its hydrophilic nature (log P: 0.49), as it exists mainly in a zwitterionic form at physiological pH. Topical delivery may enhance patient compliance by avoiding first-pass metabolism and gastrointestinal disturbances associated with oral administration while enabling direct delivery to the target site.

Niosomes are ultra-deformable nanovesicular carriers composed of cholesterol and non-ionic surfactants such as Span. They have attracted considerable interest among nanocarriers because of their excellent flexibility, biocompatibility, enhanced stability, and ability to encapsulate both hydrophilic and lipophilic drugs. Therefore, after topical application, niosomes may improve the permeation and absorption of hydrophilic drugs.

Considering these advantages, the present investigation aimed to apply a Quality by Design (QbD) approach with design of experiments (DOE)-based optimization to develop an FEX HCl niosomal gel. Attempts were made to identify the quality target product profile (QTPP) and critical quality attributes (CQAs) of the FEX HCl niosomal gel intended for topical delivery in the management of chronic idiopathic urticaria (CIU). In niosomal preparation, cholesterol enhances bilayer stability and rigidity, whereas Span 60 forms stable niosomal vesicles with high drug entrapment. The resulting formulation produced a consistent, uniform, milky-white colloidal dispersion, indicating the formation of spherical vesicles with intact bilayer membranes.

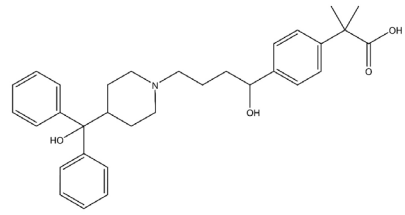
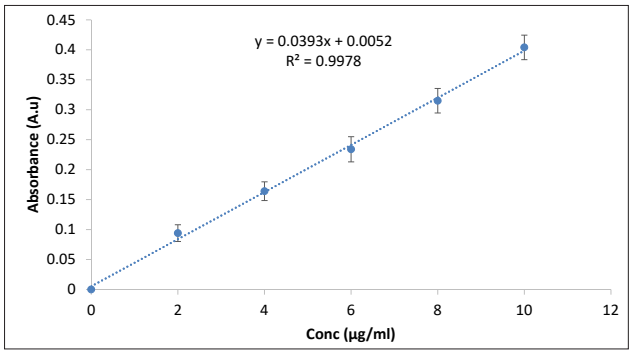


Figure 2. Structure of fexofenadine hydrochloride

Calibration curve of fexofenadine hydrochloride

The standard curve of FEX HCl was linear over the concentration range of 2-10 µg/mL. The calibration curve is shown in Figure 3. The curve showed a slope value of 0.0357 and an R^2 value of 0.9913, indicating good

linearity. The slope of the standard curve was used to determine the drug content and the *in vitro* diffusion data of FEX HCl from the niosomal gel.



All values are expressed as mean ± SD (n = 3)

Figure 3. Calibration curve of fexofenadine hydrochloride

Experimental design

Design of experiments (DOE) was used to develop and optimize the topical niosomal formulation with the minimum number of experimental trials. To evaluate the effects of important formulation variables, a 2^3 full factorial design was selected, resulting in eight experimental runs (Table 4). A linear model was fitted to the obtained responses, and ANOVA and R^2 analysis were used to verify the validity of the generated mathematical model.

Table 4. Observed responses prepared for fexofenadine-loaded niosome batches

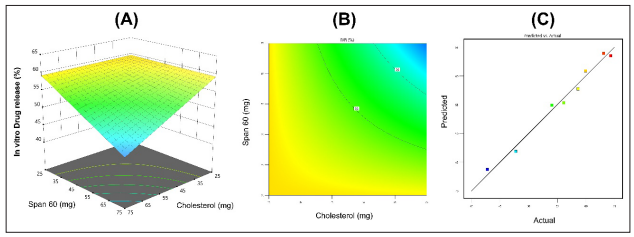
Runs	Dependent Variable	
	Y1 (%)	Y2 (%)
1	77.32±0.20	64.32±0.24
2	53.67±0.16	56.15±0.32
3	60.00±0.39	42.8±0.25
4	75.34±0.22	59.97±0.07
5	74.34±0.21	58.65±0.23
6	56.21±0.08	54.07±0.36
7	68.00±0.38	47.75±0.36
8	76.09±0.06	63.11±0.51

All values in the table are expressed as mean±SD (n=3)

Entrapment efficiency

Cholesterol was found to have a predominant negative effect on %EE, whereas Span 60 showed a positive effect. The %EE increased when the concentration of Span 60 (B) was increased, ranging from 53.67 ± 0.16% to 77.32 ± 0.20%, as indicated by the 3D response surface and contour plots (Figure 4). This increase may be explained by the properties of Span 60, which promotes the formation of a rigid and stable niosomal bilayer, thereby increasing drug entrapment.

The positive slope in the response surface and the closely spaced contour lines suggest a considerable favorable effect of Span 60 on %EE. Higher %EE values were observed at the highest levels of Span 60, as shown in the contour plots. The significant polynomial model ($p < 0.05$) further supported this effect, demonstrating the critical role of Span 60 in increasing EE%.

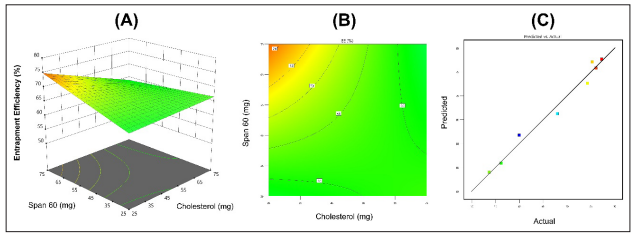


(A) 3D response surface plots of Y1, (B) contour plots for Y1, (C) predicted versus actual plots

Figure 4. Effect of independent variables on percentage entrapment efficiency (Y1)

In vitro drug release

The 3D response surface and contour plots demonstrated the combined effect of cholesterol and Span 60 on cumulative *in vitro* drug release (IVR%) at 8 h, while factor C was kept constant. IVR ranged from 42.80% to 64.32% (Figure 5). The plots clearly indicated that increasing the concentrations of the two variables led to a significant reduction in drug release, as shown by the downward slope of the response surface and the shift of the contour lines toward lower IVR% values. This reduction was mainly attributed to the formation of a rigid and stable niosomal bilayer, which decreased membrane permeability and thereby slowed drug diffusion. Both ingredients contributed to reduced drug release by further stabilizing the bilayer. The quadratic polynomial model describing IVR% was statistically significant ($p < 0.05$), with Span 60 showing a highly significant negative effect ($p < 0.01$), confirming its dominant role in controlling drug release.



(A) 3D response surface plots of Y2, (B) contour plots for Y2, and (C) predicted versus actual plots

Figure 5. Effect of independent variables on percentage drug release at 8 h (Y2)

Overlay plot

The desirability plot represents the combined effect of two independent variables, X1 and X2, on the selected responses, namely %EE and *in vitro* release percentage (IVR%), while X3 was kept constant at 5 (Table 5).

Table 5. Results of regression analysis and polynomial coefficients relating to each Critical parameters attribute (CPA)

Response	F-value	*p*-value	R^2	Adjusted R^2
Y1: EE (%)	20.22	0.0478	0.9806	0.9321
Y2: DR at the end of 8h%	13.15	0.0303	0.9460	0.8741
Regression equation of the fitted model				
Y1 = 67.62 – 2.24A + 1.80B + 4.32C – 3.18AB – 6.57BC (3)				
Y2 = 55.85 – 3.62A – 3.56B – 3.40AB – 2.93BC (4)				

A higher desirability value, close to 1, is desirable because it indicates better predictability of the generated

mathematical models (Figure 6). Higher desirability values were observed at lower levels of Span 60 and low to intermediate levels of cholesterol. In contrast, desirability decreased considerably at higher levels of Span 60. The highlighted point, corresponding to approximately X1 = 66 mg and X2 = 25 mg, showed predicted responses of EE ≈ 77.3% and IVR ≈ 62.2%, indicating an optimized formulation region that satisfied both response constraints.

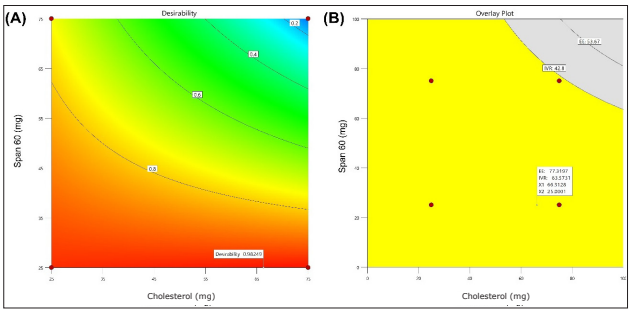


Figure 6. Overlay plot showing the combined effect of independent variables on (A) EE% and (B) *in vitro* drug release.

The optimized niosomal suspension (Run 9) showed entrapment efficiency and *in vitro* release values that closely matched the predicted results. Low prediction errors (< 1.0%) confirmed the validity of the polynomial regression models (Table 6), demonstrating the robustness and reliability of the optimization strategy.

Table 6. Predicted and experimental values of the optimized niosomal formulation

Run	Optimal settings	Response	Experimental value	Predicted value	Prediction error (%)
#9	X1 = 66 mg X2 = 25 mg X3 = 5 min	Y1: EE (%)	77.32 ± 0.20	77.65	0.327
		Y2: %DR at 8 h	63.57 ± 2.21	63.50	0.110

X1 - cholesterol; X2 - Span 60; X3 - sonication time

Particle size, polydispersity index, and zeta potential

The optimized FEX HCl-loaded niosomal formulation had a particle size of 160 ± 7.3 nm. The particle size distribution of the optimized formulation is shown in Figure 7A. The size distribution was polydisperse, as indicated by a PDI value of 0.55 ± 0.03.

The zeta potential distribution of the FEX HCl-loaded niosomes is shown in Figure 7B. The formulation showed a negative zeta potential of −28.9 ± 5.5 mV, indicating adequate stability of the colloidal carrier. The negative charge may be attributed to the presence of Span 60 and cholesterol in the niosomal bilayer.

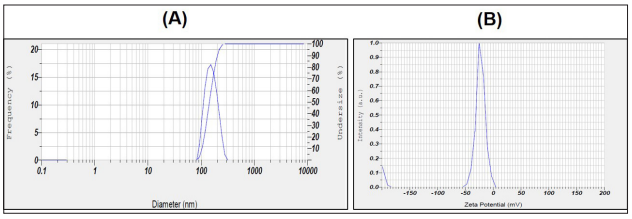


Figure 7. The optimized fexofenadine hydrochloride-loaded niosomes (A) Particle size and (B) Zeta potential

Fourier transform infrared spectroscopy and differential scanning calorimetry

FT-IR spectroscopy was used to assess potential drug-excipient interactions in the pure drug, individual excipients, physical mixture, and optimized niosomal formulation. FEX HCl showed characteristic peaks at 3400 cm^{-1} (O–H stretching), 2922 cm^{-1} (aliphatic C–H stretching), 1700 cm^{-1} (C=O stretching), and 1600 cm^{-1} (aromatic C=C stretching), confirming drug integrity. Span 60 exhibited characteristic peaks at 2850 cm^{-1} (C–H stretching) and 1735 cm^{-1} (ester C=O stretching), indicating its ester-based surfactant nature. Cholesterol showed peaks at 3400 cm^{-1} (O–H stretching), 2930 cm^{-1} (C–H stretching), and 1150 cm^{-1} (C–O stretching), confirming its structure.

The physical mixture showed peaks at 3400 cm^{-1}, 2920-2850 cm^{-1}, 1721 cm^{-1}, and 1600 cm^{-1}, indicating the absence of chemical interactions. The niosomal formulation exhibited peaks at 3380 cm^{-1}, 2920 cm^{-1}, 1730 cm^{-1}, and 1600 cm^{-1}, with slightly reduced intensity, suggesting physical entrapment of the drug without incompatibility. The absence of major chemical interactions and the high compatibility of the formulation components were confirmed by the FT-IR spectra of the physical mixture (Figure 8A), which showed the characteristic peaks of FEX HCl at similar wavenumbers.

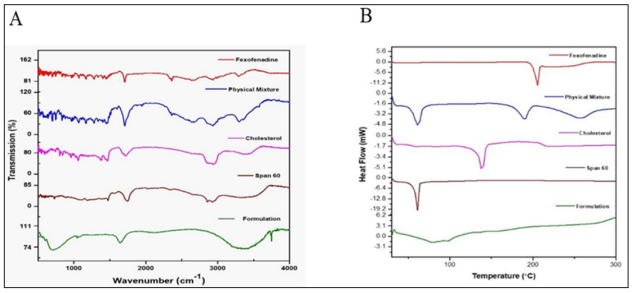


Figure 8. FT-IR spectra and chemical structures (A), and DSC thermograms of fexofenadine hydrochloride, physical mixture, cholesterol, Span 60, and optimized fexofenadine hydrochloride niosomal formulation (B).

DSC analysis was performed for the pure FEX HCl, excipients, physical mixture, and niosomal formulation (Figure 8B). FEX HCl showed a sharp endothermic peak at 196°C, corresponding to its melting point and confirming its crystalline nature. Span 60 exhibited a distinct endothermic peak at 53°C, indicating its melting point. Cholesterol showed an endothermic peak at 145°C. The physical mixture exhibited peaks at 52°C, 148°C, and 198°C, with slight shifts, indicating reduced crystallinity of FEX HCl.

The niosomal formulation showed broadening and disappearance of the drug melting peak at 195°C, suggesting a further reduction in crystallinity and successful entrapment of FEX HCl within the niosomal bilayer.

X-ray diffraction

The absence of any visible peak in the niosomal sample spectrum indicates that FEX HCl and other crystalline structures were present in the amorphous state. Figure 9 displays the XRD spectra of cholesterol, Span 60, FEX HCl and freeze-dried niosome powder. Several sharp peaks were observed at 12.5°, 14.8°, 16.2°, 18.1°, 19.4°, and 21.7°. XRD diffraction analysis of free FEX HCl and the other excipients confirmed their crystalline structure, with the diffraction patterns showing good consistency. Span 60 displayed

a single peak at 20.5°, whereas cholesterol displayed intense peaks at 14.2° and 16.9°. 18.7°, 20.5° and 23.3°. The amorphous nature of the drug in the niosomal formulation | is noticeable as the intensity of the characteristic drug peaks is considerably reduced. These X-ray diffraction findings were consistent with the DSC data.

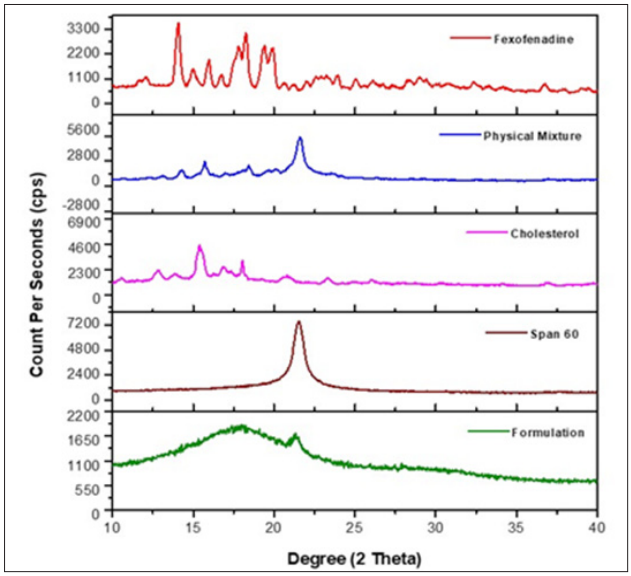


Figure 9. X-ray diffraction patterns of fexofenadine hydrochloride, physical mixture, cholesterol, Span 60, and optimized fexofenadine hydrochloride niosomal formulation

Morphology of niosomes

SEM images of the niosomes (Figure 10A) showed that the vesicles were spherical and separated from each other. The images also confirmed the nanoscale size of the niosomes. The microscopic findings were consistent with the particle size analysis data obtained using the Zetasizer.

The EDX spectrum showed characteristic elemental peaks, confirming the elemental composition of the formulation (Figure 10B). The weight percentages of the analyzed elements, including carbon, oxygen, sodium, phosphorus, sulfur, and potassium, are shown in Figure 10C. This combined SEM-EDX analysis confirmed the morphology and elemental composition of the developed formulation.

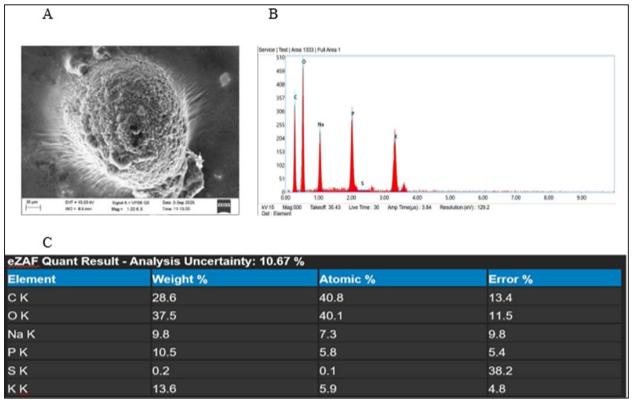


Figure 10. (A) SEM micrograph of the optimized niosomal formulation, (B) EDX spectrum of the optimized niosomal formulation, and (C) quantitative analysis of carbon, oxygen, sodium, phosphorus, sulfur, and potassium elements based on EDX analysis

Characteristics of niosomal gel

1. pH

The pH of the formulation is important in the development of topical drug delivery systems. Even small changes in the pH of a topical gel may cause skin irritation after application. The optimized niosomal gel had a pH of 6.3 ± 0.50, indicating that the FEX HCl niosomal gel is suitable for topical use because its pH is close to that of normal skin. This result is consistent with previously reported findings [29].

2. Spreadability

Spreadability plays a crucial role in the therapeutic performance of a topical formulation, as it ensures uniform and effortless application of the gel over the skin, thereby improving patient compliance. The spreadability of the optimized niosomal gel was 20.25 ± 0.81 g·cm/s. The niosomal gel exhibited satisfactory spreadability, indicating its suitability for topical use.

3. *In vitro* drug release

The *in vitro* release study performed over 8 h showed that the optimized niosomal formulation achieved cumulative drug release ranging from 42.80 ± 0.25% to 64.32 ± 0.24% (Figure 11). Niosomes are known to improve drug release and skin permeation because of their bilayer vesicular structure composed of non-ionic surfactants, nanoscale size, and increased surface area, which facilitate close contact with the skin and improve drug diffusion.

In addition, the vesicular bilayer acts as a drug reservoir, providing sustained release, protecting the drug from degradation, and increasing residence time within the skin layers. These properties make niosomes a promising carrier system for topical delivery with improved therapeutic efficacy.

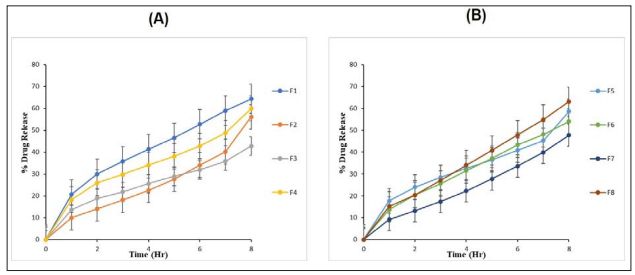


Figure 11. Comparative in vitro release from niosomal formulations: (A) F1–F4 and (B) F5–F8. Each value represents the mean ± SD (n = 3)

Analysis of the release kinetics indicates that drug release from all niosomal formulations is best described by zero-order kinetics. This is evidenced by consistently higher R^2 values (approximately 0.94-0.998) compared to first-order models (approximately 0.56-0.76). This suggests a nearly constant, concentration-independent release rate over time, which is an ideal characteristic for controlled topical delivery (Table 7). The comparatively lower fit to the first-order model confirms that release is not predominantly driven by concentration gradients. The Higuchi model also shows high correlation coefficients (approximately 0.85-0.98), indicating

Table 7. Regression coefficient of various mathematical models for the release of all formulations

Run	Zero order		First Order		Korsmeyer-Peppas			Higuchi	
	K value	R^2	K value	R^2	K value	n value	R^2	K value	R^2
1	7.14±0.01	0.962±0.015	0.35±0.03	0.762±0.173	6.33±0.02	1.989±0.64	0.774±0.166	18.11±0.02	0.968±0.052
2	6.08±0.03	0.961±0.003	0.38±0.05	0.746±0.002	3.73±0.03	0.922±0.65	0.745±0.070	17.53±0.03	0.861±0.003
3	4.52±0.02	0.945±0.002	0.32±0.02	0.596±0.003	4.82±0.01	1.121±0.003	0.609±0.004	14.03±0.01	0.981±0.001
4	6.21±0.01	0.943±0.001	0.34±0.01	0.579±0.004	5.77±0.04	1.200±0.004	0.592±0.005	19.20±0.02	0.965±0.0017
5	5.98±0.02	0.937±0.0008	0.34±0.04	0.581±0.0009	5.62±0.03	1.183±0.002	0.5905±0.001	18.40±0.03	0.955±0.001
6	6.27±0.01	0.979±0.003	0.36±0.02	0.640±0.006	4.83±0.01	1.263±0.006	0.662±0.006	19.05±0.04	0.975±0.003
7	5.57±0.04	0.992±0.0008	0.37±0.02	0.741±0.002	3.58±0.02	1.283±0.006	0.749±0.004	16.28±0.01	0.914±0.003
8	6.87±0.03	0.992±0.004	0.20±0.01	0.768±0.179	13.6±0.01	1.104±0.351	0.955±0.010	26.35±0.02	0.955±0.010

Each value represents the mean ± SD (n = 3)

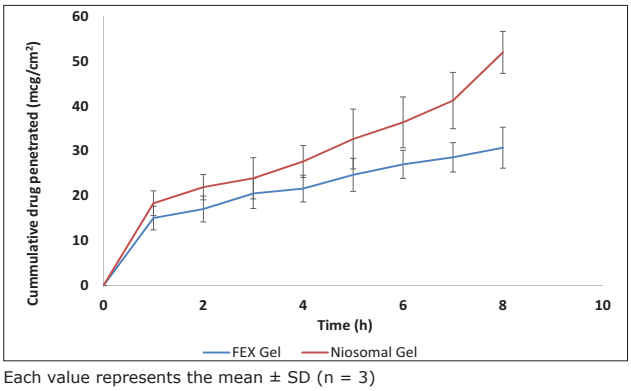
that drug release is significantly governed by diffusion from the vesicular matrix.

Furthermore, the Korsmeyer-Peppas model sheds light on the release mechanism. The diffusional exponent (n-value ranging from ~0.58 to 1.29 across formulations) suggests a blend of anomalous (non-Fickian) transport involving diffusion and the relaxation/erosion of the niosomal bilayer. The optimised formulation (e.g. F5/F8, based on the highest R^2 and release profile) demonstrates a strong fit to the zero-order and Higuchi models, as well as Peppas 'n' values that are indicative of controlled, sustained release via diffusion-coupled relaxation mechanisms. This confirms that the niosomal system acts as an effective reservoir, ensuring prolonged and predictable drug release, which is suitable for enhanced topical therapeutic performance.

4. *Ex vivo* permeation study

The *ex vivo* permeation profile, expressed as the cumulative percentage of drug permeated versus time, showed a time-dependent increase in drug absorption for both formulations. However, the optimized niosomal gel consistently exhibited significantly higher permeation than the control gel (FEX gel) at all sampling intervals.

At 1 h, the niosomal gel showed approximately 18% drug permeation, whereas the FEX gel showed approximately 15%, indicating an early enhancement effect. This difference became progressively more pronounced over time, with the niosomal gel achieving 51.97 ± 0.40% cumulative permeation at 8 h, compared with only 30.00 ± 0.28% for the FEX gel (Figure 12).



Each value represents the mean ± SD (n = 3)

Figure 12. *Ex vivo* permeation profile of FEX HCl and optimised niosomal gel

The enhanced permeation from the niosomal formulation may be attributed to its nanosized vesicular structure, which facilitates closer interaction with the stratum corneum, improves drug partitioning, and enhances diffusion across skin layers. Statistical analysis using an unpaired Student's t-test confirmed that the difference in permeation between the two formulations was statistically significant ($p < 0.05$), thereby demonstrating the superior permeation efficiency of the niosomal gel compared with the conventional gel system.

CONCLUSION

Fexofenadine hydrochloride-loaded niosomes were successfully developed using the ethanol injection method to achieve efficient topical delivery. Optimization was performed using a 2^3 factorial design. The optimized formulation exhibited nanoscale particle size, a low polydispersity index, and good colloidal stability. Scanning electron microscopy confirmed the spherical morphology of the nanosized niosomes. Differential scanning calorimetry and X-ray diffractometry confirmed the amorphous state of the drug within the niosomal bilayer.

Furthermore, the niosomal gel containing fexofenadine hydrochloride showed suitable spreadability and an appropriate pH for topical application. *Ex vivo* skin permeation studies confirmed an approximately two-fold increase in permeation from the fexofenadine hydrochloride-loaded niosomal gel compared with the control gel. In conclusion, fexofenadine hydrochloride can be effectively formulated in niosomal vesicles for topical delivery in the management of chronic idiopathic urticaria.

ABBREVIATIONS

FEX HCl – fexofenadine hydrochloride
CIU – chronic idiopathic urticaria
CSU – chronic spontaneous urticaria
UV – ultraviolet
PDI – polydispersity index
DLS – dynamic light scattering
FT-IR – Fourier transform infrared spectroscopy
XRD – X-ray diffraction
DSC – differential scanning calorimetry
SEM – scanning electron microscopy

EDX – energy-dispersive X-ray spectroscopy
QbD – Quality by Design
QTPP – quality target product profile
CQAs – critical quality attributes
EE – entrapment efficiency
ANOVA – analysis of variance
IVR – *in vitro* release
PBS – phosphate-buffered saline
q.s. – quantity sufficient

CONFLICT OF INTEREST:

The authors declare no conflict of interest.

ORCID iDs

H.S. Lavanya https://orcid.org/0009-0000-3980-5533
H.N. Shivakumar https://orcid.org/0000-0003-1596-9941
Bindu Banakar https://orcid.org/0009-0003-0608-3310
Rushikesh Shinde https://orcid.org/0009-0003-0304-3057

REFERENCES

1. Doong JC, Chichester K, Oliver ET, Schwartz LB, Saini SS. Chronic idiopathic urticaria: systemic complaints and their relationship with disease and immune measures. *J Allergy Clin Immunol Pract*. 2017;5(5):1314-8. doi:10.1016/j.jaip.2016.11.037.
2. Kozel MM, Mekkes JR, Bossuyt PM, Bos JD. The effectiveness of a history-based diagnostic approach in chronic urticaria and angioedema. *Arch Dermatol*. 1998;134(12):1575-80.
3. Grattan CE, Sabroe RA, Greaves MW. Chronic urticaria. *J Am Acad Dermatol*. 2002;46(5):645-60.
4. Shah HS, Gotecha A, Jetha D, Rajput A, Bariya A, Panchal S, et al. Gamma oryzanol niosomal gel for skin cancer: formulation and optimization using quality by design (QbD) approach. *AAPS Open*. 2021;7:9. doi:10.1186/s41120-021-00041-2.
5. Nasr AM, Qushawy MK, Elkhoudary MM, Gawish AY, Elhady SS, Swidan SA. Quality by design for development of enhanced *in situ* forming vesicles for improving bioavailability of fexofenadine HCl *in vitro* and *in vivo*. *Pharmaceutics*. 2020;12(5):409.
6. Batool M, Zamir A, Alqahtani F, Ahmad T, Saeed H, Rasool MF. Clinical pharmacokinetics of fexofenadine: a systematic review. *Pharmaceutics*. 2024;16(12):1619. doi:10.3390/pharmaceutics16121619.
7. Caparica R, Júlio A, Rosado C, Santos de Almeida T. Applicability of ionic liquids in topical drug delivery systems: a mini review. *J Pharmacol Clin Res*. 2018;4(5):555649.
8. Aishwarya KS, Ananya MS, Anjana NK. A review on topical gels as drug delivery system. *J Pharma Insights Res*. 2024;2(4):218-22.
9. Riccardi D, Baldino L, Reverchon E. Liposomes, transferosomes and niosomes: production methods and applications in the vaccinal field. *J Transl Med*. 2024;22(1):339.
10. Abdelhameed AH, Abdelhafez WA, Mohamed MS. Formulation, optimization, and *in vivo* evaluation of nanostructured lipid carriers loaded with fexofenadine HCl for oral delivery. *J Drug Deliv Sci Technol*. 2022;74:103607.
11. Liga S, Paul C, Moacă EA, Peter F. Niosomes: composition, formulation techniques, and recent progress as delivery systems in cancer therapy. *Pharmaceutics*. 2024;16(2):223.
12. Breier AR, Steppe M, Schapoval EE. Validation of UV spectrophotometric method for fexofenadine HCl in pharmaceutical formulations and comparison with HPLC. *Anal Lett*. 2007;40(12):2329-37.
13. Estupiñan OR, Garcia-Manrique P, Blanco-Lopez MDC, Matos M, Gutiérrez G. Vitamin D3-loaded niosomes and transferosomes produced by ethanol injection method: identification of the critical preparation step for size control. *Foods*. 2020;9(10):1367.
14. Mohsen AM, El-Hashemy HA, Salama A, Darwish AB. Formulation of tizanidine hydrochloride-loaded provesicular system for improved oral delivery employing a 2^3 full factorial design. *Drug Deliv Transl Res*. 2023;13(2):580-92.
15. Aldawsari MF, Khafagy ES, Moglad EH, Lila AS. Formulation optimization, *in vitro* and *in vivo* evaluation of niosomal nanocarriers for enhanced topical delivery of cetirizine. *Saudi Pharm J*. 2023;31(9):101734.
16. Revankar AA, Patil AS, Karishetti R, Chougule KR, Patil P, Salokhe A. Enhanced bioavailability of quercetin-loaded niosomal *in situ* gel for management of Parkinson's disease. Front Pharmacol. 2025;15:1519649.
17. Eldeeb AE, Salah S, Amer MS, Elkasabgy NA. 3D nanocomposite alginate hydrogel loaded with pitavastatin nanovesicles as a functional wound dressing with controlled drug release: preparation, *in vitro* and *in vivo* evaluation. *J Drug Deliv Sci Technol*. 2022;71:103292.
18. Tamaddon L, Mohamadi N, Bavarsad N. Preparation and characterization of mucoadhesive loratadine nanoliposomes for intranasal administration. *Turk J Pharm Sci*. 2021;18(4):492-7.
19. Gaikwad DS, Chougale RD, Patil KS, Disouza JI, Hajare AA. Design, development, and evaluation of docetaxel-loaded niosomes for the treatment of breast cancer. *Future J Pharm Sci*. 2023;9(1):43.
20. Nanjappa SH, Somasekhar V, Kamath M, Prakash SS, Kumar A, Pai R, et al. Formulation and evaluation of isosorbide dinitrate-loaded flash-release dispersible sublingual wafers. *RSC Pharm*. 2026.
21. Maghsoodi M, Tajalli Bakhsh AS. Evaluation of physico-mechanical properties of drug-excipient agglomerates obtained by crystallization. *Pharm Dev Technol*. 2011;16(3):243-9.
22. Vuddanda PR, Montenegro-Nicolini M, Morales JO, Velaga S. Effect of plasticizers on physico-mechanical properties of pullulan-based pharmaceutical oral films. *Eur J Pharm Sci*. 2017;96:290-8.
23. Evrard Q, Houard F, Daiguebonne C, Calvez G, Suffren Y, Guillou O, et al. Sonocrystallization as an efficient way to control the size, morphology, and purity of coordination compound microcrystallites: application to a single-chain magnet. *Inorg Chem*. 2020;59(13):9215-26.
24. Danafar H, Maleki MN, Moradi AH, Sharafi A, Nedaei K. Preparation and characterization of niosomes containing silver nanoparticles as a radiosensitizer for enhancing radiotherapy of lung cancer. *Sci Rep*. 2025;15(1):14964.
25. Shah A, Boldhane S, Pawar A, Bothiraja C. Advanced development of a non-ionic surfactant and cholesterol material based niosomal gel formulation for the topical delivery of anti-acne drugs. *Mater Adv*. 2020;1(6):1763-74.
26. Veni MR, Mandati N, Mamidipalli A, Raghavarapu P, Tirunagari M. Formulation and *in vitro* evaluation of niosomal gel for the topical administration of losartan potassium. *J Drug Deliv Ther*. 2024;14(1).
27. Sguizzato M, Pepe A, Baldisserotto A, Barbari R, Montesi L, Drechsler M, et al. Niosomes for topical application of antioxidant molecules: design and *in vitro* behavior. *Gels*. 2023;9(2):107.
28. Bhardwaj S, Bhatia S. Development and characterization of niosomal gel system using Lallementia royaleana Benth. mucilage for the treatment of rheumatoid arthritis. *Iran J Pharm Res*. 2020;19(3):465.
29. Waqas MK, Sadia H, Khan MI, Omer MO, Siddique MI, Qamar S, et al. Development and characterization of niosomal gel of fusidic acid: *in-vitro* and *ex-vivo* approaches. *Des Monomers Polym*. 2022;25(1):165-74. doi:10.1080/15685551.2022.2086411.